THE JOURNAL OF BIOLOGICAL CHEMISTRY VOL. 286, NO. 6, pp. 4341–4348, February 11, 2011

Caveolin-1 Assembles Type 1 Inositol 1,4,5-Trisphosphate Receptors and Canonical Transient Receptor Potential 3 Channels into a Functional Signaling Complex in Arterial Smooth Muscle Cells*

Received for publication, August 27, 2010, and in revised form, October 23, 2010 Published, JBC Papers in Press, November 23, 2010, DOI 10.1074/jbc.M110.179747

Adebowale Adebiyi, Damodaran Narayanan, and Jonathan H. Jaggar[1]

From the Department of Physiology, University of Tennessee Health Science Center, Memphis, Tennessee 38163

Physical coupling of sarcoplasmic reticulum (SR) type 1 inositol 1,4,5-trisphosphate receptors (IP_3R1) to plasma membrane canonical transient receptor potential 3 (TRPC3) channels activates a cation current (I_{Cat}) in arterial smooth muscle cells that induces vasoconstriction. However, structural components that enable IP_3R1 and TRPC3 channels to communicate locally are unclear. Caveolae are plasma membrane microdomains that can compartmentalize proteins. Here, we tested the hypothesis that caveolae and specifically caveolin-1 (cav-1), a caveolae scaffolding protein, facilitate functional IP_3R1 to TRPC3 coupling in smooth muscle cells of resistance-size cerebral arteries. Methyl-β-cyclodextrin (MβCD), which disassembles caveolae, reduced IP_3-induced I_{Cat} activation in smooth muscle cells and vasoconstriction in pressurized arteries. Cholesterol replenishment reversed these effects. Cav-1 knockdown using shRNA attenuated IP_3-induced vasoconstriction, but did not alter TRPC3 and IP_3R1 expression. A synthetic peptide corresponding to the cav-1 scaffolding domain (CSD) sequence (amino acids 82–101) also attenuated IP_3-induced I_{Cat} activation and vasoconstriction. A cav-1 antibody co-immunoprecipitated cav-1, TRPC3, and IP_3R1 from cerebral artery lysate. ImmunoFRET indicated that cav-1, TRPC3 channels and IP_3R1 are spatially co-localized in arterial smooth muscle cells. IP_3R1 and TRPC3 channel spatial localization was disrupted by MβCD and a CSD peptide. Cholesterol replenishment re-established IP_3R1 and TRPC3 channel close spatial proximity. Taken together, these data indicate that in arterial smooth muscle cells, cav-1 co-localizes SR IP_3R1 and plasma membrane TRPC3 channels in close spatial proximity thereby enabling IP_3-induced physical coupling of these proteins, leading to I_{Cat} generation and vasoconstriction.

Several G-protein-coupled receptor agonists activate phospholipase C leading to generation of the second messenger, inositol 1,4,5-trisphosphate (IP_3)[2] (1). IP_3 binds to endo/sarcoplasmic reticulum-localized IP_3 receptors leading to Ca^{2+} release from the endo/sarcoplasmic reticulum (2). In arterial smooth muscle cells, the resultant increase in intracellular Ca^{2+} concentration ($[Ca^{2+}]_i$) causes vasoconstriction. IP_3 also activates a non-selective cation current (I_{Cat}), leading to vasoconstriction (3–7). IP_3-induced I_{Cat} activation occurs independently of sarcoplasmic reticulum (SR) Ca^{2+} release and due to a physical interaction between type 1 IP_3 receptors (IP_3R1) and canonical transient receptor potential (TRPC) 3 channels (4–6). IP_3R1 selectively couples to TRPC3 channels due to close spatial proximity of these proteins (4). A wide variety of signal transduction pathways require interacting molecules to form functional macromolecular complexes. These complexes often contain one or more scaffolding proteins that traffic, localize, or compartmentalize signaling molecules (8). However, whether scaffolding proteins are required to assemble IP_3R1 and TRPC3 channels into a functional macromolecular complex in arterial smooth muscle cells is unclear.

Caveolae are plasma membrane microdomains that act as compartments for several signal transduction molecules, including receptors, ion channels, and scaffolding proteins (9). Caveolae integrity is sustained by cholesterol and caveolin proteins, of which there are three different isoforms (cav-1–3). Caveolin isoforms can exhibit tissue-specific expression (9). Cav-1 is required for caveolae formation in arterial smooth muscle cells, embryonic fibroblasts, lung endothelial, and epithelial cells (10–13). Cav-1 ablation and caveolae disruption attenuate both pressure- and agonist-induced vasoconstriction, indicating that caveolae play an important role in the regulation of vascular reactivity (11, 14–17). In arterial smooth muscle cells, peripheral SR membrane can be located nearby plasma membrane caveolae (16). This close spatial proximity may permit or enhance interactions between SR- and caveolae-localized plasma membrane proteins. Whether IP_3R1, TRPC channels, and caveolin proteins physically and functionally interact in arterial smooth muscle cells is unclear.

* This work was supported, in whole or in part, by National Institutes of Health NHLBI Grants R01 HL67061 and HL094378 (to J. H. J.), and K01 HL096411 (to A. A.).

[1] To whom correspondence should be addressed: 894 Union Ave., Memphis TN 38163. Tel.: 901-448-1208; Fax: 901-448-7126; E-mail: jjaggar@uthsc.edu.

[2] The abbreviations used are: IP_3, inositol 1,4,5-trisphophate; IP_3R, inositol 1,4,5-trisphosphate receptors; TRPC, canonical transient receptor potential; SR, sarcoplasmic reticulum; Cav-1, caveolin-1; Cav-1scrm, vectors encoding caveolin-1 scrambled short hairpin RNA; Cav-1shV, vectors encoding caveolin-1 short hairpin; Bt- IP_3, 2,3,6-tri-*O*-butyryl-*myo*-inositol 1,4,5-trisphosphate-hexakis (propionoxymethyl) ester; MβCD, methyl β-cyclodextrin; Chol/MβCD, cholesterol-loaded methyl β-cyclodextrin; CSD, caveolin-1 scaffolding domain peptide; *ANT*, *antennapedia*; ANT-CSD, caveolin-1 scaffolding domain peptide-labeled *antennapedia*; FITC, fluorescein isothiocyanate; ANT-FITC, FITC-labeled *antennapedia*; immunoFRET, immunofluorescence resonance energy transfer; N-FRET, normalized FRET.

In the present study, we examined the significance of caveolae in mediating IP_3-induced I_{Cat} activation in cerebral artery smooth muscle cells and vasoconstriction in pressurized cerebral arteries. We show that caveolae disassembly using cyclodextrin, cav-1 knockdown using RNAi, or a cav-1 scaffolding domain (CSD) peptide that competes with endogenous *cav*-1 for interacting protein binding, inhibit IP_3-induced I_{Cat} activation in smooth muscle cells and vasoconstriction. Data indicate that IP_3R1 and TRPC3 physically interact with cav-1, and that cav-1 and caveolae maintain plasma membrane TRPC3 and SR IP_3R1 in a functional signaling complex in cerebral artery smooth muscle cells, thereby permitting IP_3-induced vasoconstriction.

EXPERIMENTAL PROCEDURES

Tissue Preparation and Smooth Muscle Cell Isolation—Animal protocols used were reviewed and approved by the Animal Care and Use Committee at the University of Tennessee Health Science Center. Male Sprague-Dawley rats (6–8 weeks) were euthanized by intraperitoneal injection of sodium pentobarbital (150 mg/kg). The brain was removed and resistance-size cerebral arteries (posterior cerebral, cerebellar, and middle cerebral, <200 μm) were harvested and maintained in ice-cold (4 °C), oxygenated (21% O_2-5% CO_2-74% N_2) physiological saline solution (PSS) containing (in mM): 119 NaCl, 4.7 KCl, 24 $NaHCO_3$, 1.2 KH_2PO_4, 1.6 $CaCl_2$, 1.2 $MgSO_4$, and 11 glucose (pH 7.4). Individual smooth muscle cells were dissociated from cerebral arteries using a HEPES-buffered solution containing (in mM): 55 NaCl, 80 sodium glutamate, 5.6 KCl, 2 $MgCl_2$, 10 HEPES, and 10 glucose (pH 7.3), as previously described (18) Briefly, cerebral arteries were placed into isolation solution containing 0.7 mg/ml papain, 1 mg/ml dithioerythreitol, and 1 mg/ml bovine serum albumin (BSA) for 12 min at 37 °C. Arteries were then immediately transferred to isolation solution containing 1 mg/ml collagenase F and H (2:1), 100 μM $CaCl_2$, and 1 mg/ml BSA for 10 min at 37 °C. Arteries were subsequently washed in isolation solution and triturated using a fire-polished glass pipette to yield single smooth muscle cells. Cells were maintained at 4 °C, and used for experimentation within 8 h.

Patch-Clamp Electrophysiology—Membrane currents and cell capacitance were measured in isolated smooth muscle cells using the patch-clamp technique (Axopatch 200B, Clampex 8.2). I_{Cat} was measured using the conventional whole cell patch-clamp configuration, as we have done previously (5, 6). Briefly, whole cell currents were measured by applying 940-ms voltage ramps between −120 and + 20 mV from a holding potential of −40 mV. Bath solution for conventional whole-cell experiments contained (in mM): 140 NaCl, 1.8 $CaCl_2$, 1.2 $MgCl_2$, 10 HEPES, and 10 glucose (pH 7.4). The pipette solution contained (in mM): 140 CsCl, 10 HEPES, 10 glucose, 5 Mg-ATP, and 5 EGTA (with pH adjusted to 7.2 with CsOH), and 100 nM free Ca^{2+}.

Pressurized Artery Diameter Measurement—Arterial diameter was measured using pressurized artery myography, as previously described (19). Briefly, an arterial segment 1–2 mm in length was cannulated at each end in a pressurized artery chamber (Living Systems Instrumentation; Burlington, VT). The chamber was continuously perfused with PSS equilibrated with a mixture of 21% O_2, 5% CO_2, 74% N_2, and maintained at 37 °C. Arterial endothelium was denuded by introducing air bubbles into the artery lumen for 1 min followed by a wash with PSS. Intravascular pressure was changed using an attached reservoir and monitored using a pressure transducer. Pressurized arteries were observed with a charge-coupled device camera attached to an inverted microscope (Nikon TE 200). Arterial diameter was measured at 1 Hz using the automatic edge-detection function of IonWizard software (Ionoptix; Milton, MA). Pharmacological agents were applied via chamber perfusion after arteries had developed steady-state spontaneous myogenic tone. Myogenic tone (%) was calculated as (1 − active diameter/passive diameter) × 100.

Cav-1 Knockdown—Using pRNA-U6.1/Neo as a template, silencing vectors were constructed to express short hairpin (sh) RNA (GenScript Corp, Piscataway, NJ) as previously described (5). Expressed DNA sequences were as follows: cav-1shV1: AAGCATCTCAACGACGACGTG, cav-1shV2: AAGACTGCAGATAGGCCTTTG, cav-1scrm: GCACACGAAGCCATCAGTTGA. The two silencing vectors (cav-1shV1 + cav-1shV2; cav-1shV) or a scrambled control (cav-1scrm) shRNA were inserted into cerebral artery segments using a reversible permeabilization procedure, as previously described (20). Arteries were placed into serum-free Dulbecco's modified Eagle's medium (DMEM) supplemented with 1% penicillin/streptomycin and incubated at 37 °C (95% O_2, 5% CO_2) for 4 days.

Co-immunoprecipitation and Western Immunoblotting—Arterial lysate (yielding ~1.5 mg total protein) was harvested from cerebral arteries using ice-cold non-denaturing lysis buffer (Thermo Scientific, Rockford, IL). Because of the small size (<200 μm diameter) of the cerebral arteries used in this study, arteries pooled from ~15 rats were required for each co-IP experiment. Co-immunoprecipitation (co-IP) was done using the Thermo Scientific Pierce co-IP kit following the manufacturer's protocol. Briefly, the cav-1 antibody (Abcam) was first immobilized for 2 h using AminoLink Plus coupling resin. The resin was then washed and incubated with arterial lysate overnight. After incubation, the resin was again washed and protein eluted using elution buffer. A negative control that was provided with the IP kit to assess nonspecific binding received the same treatment as the co-IP samples, including the cav-1 antibody. In this control, the coupling resin is not amine-reactive preventing covalent immobilization of the primary antibody onto the resin. Samples were analyzed by Western blotting using rabbit polyclonal anti-cav-1 (Abcam Inc., Cambridge, MA), mouse monoclonal anti-IP_3R1 (UC Davis/NINDS/NIMH NeuroMab Facility), rabbit polyclonal anti-TRPC3 (*Alomone* Labs Ltd. Jerusalem, Israel), and horseradish peroxidase-conjugated secondary antibodies.

Western blotting was performed as previously described (4–6). Briefly, rat cerebral artery lysate protein concentrations were determined spectrophotometrically. Proteins were separated by 7.5% gradient SDS-polyacrylamide gel electrophoresis and transferred onto nitrocellulose membranes using a Mini Trans Blot Cell (Bio-Rad). Membranes were then incu-

bated with respective antibodies and developed using enhanced chemiluminescence (Thermo Scientific).

Chemical Loading—Caveolin-1 scaffolding domain peptide (CSD) was inserted into intact cerebral arteries using the chemical loading technique modified from a previously described method (14, 21). Briefly, cerebral arteries were first placed into a Ca^{2+}-free (EGTA, 10 mM), high K^+ (120 mM) solution supplemented with ATP (5 mM) at 4 °C for ~30 min. Arteries were then incubated in the presence of CSD in Mg^{2+} (2 mM)- and ATP (5 mM)-containing Ca^{2+}-free solution at 4 °C for ~2 h. Arteries were further placed in 10 mM Mg^{2+}- and ATP (5 mM)-containing Ca^{2+}-free solution at 4 °C for ~30 min, after which the solution was changed to one containing Na^+ (140 mM) and K^+ (5 mM) and maintained at room temperature for 30 min. Ca^{2+} was then added incrementally to the solution to reach a concentration of 1.8 mM. Arteries were then placed into DMEM-F12 supplemented with 1% penicillin and streptomycin overnight (37 °C, 5% CO_2) prior to use.

Immunofluorescence Resonance Energy Transfer (Immuno-FRET) and Confocal Imaging—ImmunoFRET was performed using a modified version of our previously described method (4). Briefly, paraformaldehyde-fixed cerebral artery smooth muscle cells were permeabilized with 0.1% Triton X-100 for 1 min at room temperature. Following a 1 h of incubation in PBS containing 5% bovine serum albumin (BSA), smooth muscle cells were treated overnight at 4 °C with mouse monoclonal anti-IP$_3$R1 (UC Davis/NINDS/NIMH NeuroMab Facility), sheep polyclonal anti-TRPC3 (Abcam), rabbit polyclonal anti-cav-1 (Abcam), or anti-IP$_3$R1 plus anti-TRPC3 or anti-TRPC3 plus anti-cav-1 at a dilution of 1:100 each in PBS containing 5% BSA. After a wash and block with PBS containing 5% BSA, cells were incubated for 1 h at 37 °C with secondary antibodies: Alexa 546-conjugated donkey anti-mouse for IP$_3$R1 (1:100 dilution; Invitrogen, Carlsbad, CA) and Alexa 488-conjugated donkey anti-sheep for TRPC3 (1:100 dilution; Invitrogen). For FRET measurements using TRPC3 and cav-1 primary antibodies, Alexa 546-conjugated donkey anti-sheep and Alexa 488-conjugated goat anti-rabbit secondary antibodies were used, respectively. Following wash and mount, fluorescence images were acquired using a Zeiss LSM Pascal laser-scanning confocal microscope. Alexa 488 and Alexa 546 were excited at 488 and 543 nm and emission collected at 505–530 and >560 nm, respectively. Images were acquired using a z-resolution of ~0.8 μm. Negative controls prepared by omitting primary antibodies did not exhibit fluorescence. Images were background-subtracted and normalized FRET (N-FRET) was calculated on a pixel-by-pixel basis for the entire image and in regions of interest (within the boundaries of the cell) using the Xia method (22) and Zeiss LSM FRET Macro tool version 2.5.

Fluorescein isothiocyanate (FITC)-labeled *antennapedia* peptide was inserted into smooth muscle cells of intact cerebral arteries using chemical loading procedure. FITC fluorescence was background-subtracted. Control arteries underwent the same chemical loading and culture protocol, but were not exposed to FITC-labeled *antennapedia*. FITC fluorescence was imaged using a Zeiss LSM5 Pascal laser-scanning confocal microscope. FITC was excited at 488 nm and emission collected at 505–530 nm.

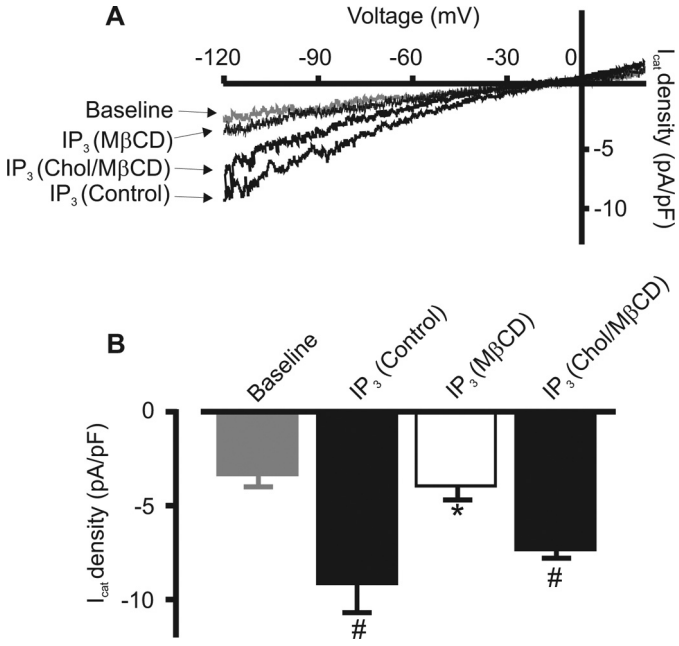

FIGURE 1. **Caveolae are required for IP$_3$-induced I$_{Cat}$ activation in cerebral artery smooth muscle cells.** *A*, representative recordings illustrating that MβCD (5 mM) inhibits IP$_3$-induced I$_{Cat}$ and reversal of this effect by further addition of Chol/MβCD (100 μg/ml). *B*, mean I$_{Cat}$ density (at −120 mV) at baseline ($n = 9$) and IP$_3$-induced I$_{Cat}$ density in control ($n = 6$), MβCD ($n = 7$), and Chol/MβCD ($n = 6$)-treated cerebral artery smooth muscle cells. *, $p < 0.05$, when compared with IP$_3$ and IP$_3$ + Chol/MβCD; #, $p < 0.05$ when compared with the baseline.

Chemicals—Unless otherwise stated, all reagents were purchased from Sigma. Papain was purchased from Worthington Biochemical (Lakewood, NJ) and 2,3,6-tri-*O*-butyryl-*myo*-inositol 1,4,5-trisphosphate-hexakis (propionoxymethyl) ester (Bt-IP$_3$) was purchased from SiChem (Bremen, Germany). Antennapedia and FITC-conjugated antennapedia peptides were purchased from Anaspec (Fremont, CA). Caveolin-1 scaffolding domain peptide was purchased from Enzo Life Sciences (Farmingdale, NY).

Statistical Analysis—Data are expressed as means ± S.E. of the mean. Statistical significance was calculated by using Student's t-tests for paired or unpaired data and analysis of variance followed by Student-Newman-Keuls post-hoc test for multiple data sets. $p < 0.05$ was considered significant.

RESULTS

Caveolae Are Required for IP$_3$-induced I$_{Cat}$ Activation in Arterial Smooth Muscle Cells and Vasoconstriction—To examine the significance of caveolae for IP$_3$-induced I$_{Cat}$ activation, freshly-isolated cerebral artery smooth muscle cells were exposed to methyl β-cyclodextrin (MβCD; 30 min), a cholesterol-depleting agent that disassembles caveolae (15, 23). MβCD treatment reduced mean smooth muscle cell capacitance (control *versus* MβCD-treated (pF): 12.1 ± 1.0, $n = 6$ *versus* 7.4 ± 1.2, $n = 7$; $p < 0.05$), consistent with a decrease in cell surface area. MβCD treatment also reduced IP$_3$-induced I$_{Cat}$ density in arterial smooth muscle cells by ~89% (Fig. 1, *A* and *B*). To study the importance of cholesterol in

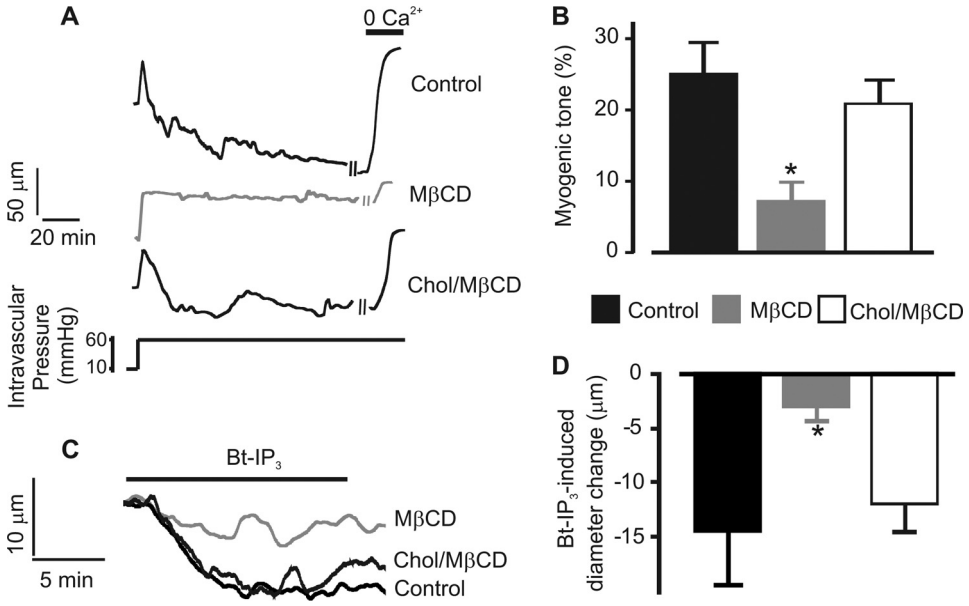

FIGURE 2. **Caveolae are required for myogenic tone and IP_3-induced vasoconstriction in cerebral arteries.** *A*, representative recordings illustrating that MβCD (10 mM) attenuates myogenic tone and reversal of this effect by Chol/MβCD (100 μg/ml). *B*, mean myogenic tone in control ($n = 6$), MβCD ($n = 6$), and Chol/MβCD ($n = 4$)-treated cerebral arteries. *C*, representative traces illustrating that MβCD (10 mM) inhibits Bt-IP_3 (10 nM)-induced vasoconstriction and reversal of this effect by Chol/MβCD (100 μg/ml). *D*, mean Bt-IP_3-induced vasoconstriction in control arteries ($n = 6$) or arteries treated with MβCD ($n = 6$), or MβCD followed by Chol/MβCD ($n = 4$). *, $p < 0.05$ when compared with the control and Chol/MβCD.

mediating this effect, cholesterol-loaded MβCD (Chol/MβCD; ~1 h) was used to replenish cholesterol in MβCD-treated arterial smooth muscle cells (15, 23, 24). Cholesterol replenishment reversed the MβCD-induced decrease in cell capacitance (to 10.7 ± 0.9 pF, $n = 6$, $p > 0.05$ when compared with control). Chol/MβCD also reversed the inhibitory effect of MβCD on IP_3-induced I_{Cat} activation (Fig. 1, *A* and *B*).

The functional significance of caveolae for IP_3-induced vasoconstriction was investigated by measuring diameter regulation of pressurized (60 mmHg), endothelium-denuded cerebral arteries. Control arteries developed ~25% mean myogenic tone (Fig. 2, *A* and *B*). MβCD treatment (2 h) reduced myogenic tone to ~7%, or by ~72% (Fig. 2, *A* and *B*). MβCD treatment also reduced vasoconstriction induced by Bt-IP_3, a membrane-permeant IP_3 analog, by ~79% (Fig. 2, *C* and *D*). Chol/MβCD treatment (~2 h) restored both myogenic tone and IP_3-induced vasoconstriction in arteries treated with MβCD (Fig. 2, *A–D*). These data suggest that intact caveolae are necessary for IP_3-induced I_{Cat} activation in arterial smooth muscle cells and myogenic tone and IP_3-induced vasoconstriction in pressurized arteries.

Cav-1 Expression Is Necessary for IP_3-induced Vasoconstriction—Cav-1 is essential for caveolae formation in cerebral artery smooth muscle cells (13). Therefore, to study the importance of cav-1 in IP_3-induced vasoconstriction, vectors encoding shRNA targeting cav-1 (cav-1shV) were inserted into cerebral arteries to suppress cav-1 expression. Western blotting indicated that cav-1shV reduced mean arterial cav-1 protein by ~41% when compared with arteries treated with scrambled shRNA (scrm; Fig. 3, *A* and *B*). In contrast, cav-1shV did not alter TRPC3 or IP_3R1 expression (Fig. 3, *A* and *B*). Cav-1 knockdown reduced myogenic tone in endothelium-denuded pressurized (60 mmHg) arteries by ~50% (Fig. 4, *A* and *B*). Cav-1 knockdown also reduced Bt-IP_3-induced vasoconstriction by ~ 61% (Fig. 4, *C* and *D*). These data indicate that cav-1 expression is required for myogenic tone and IP_3-induced vasoconstriction in cerebral arteries.

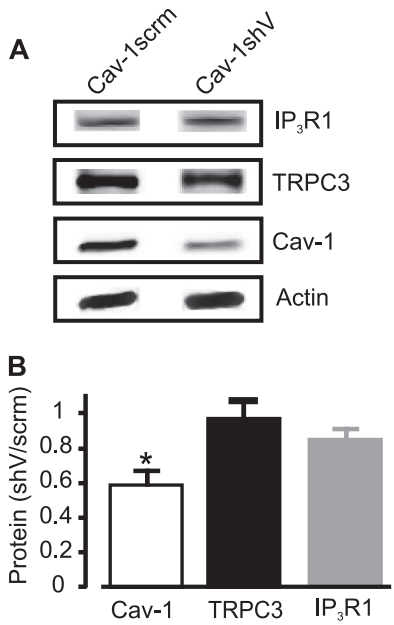

FIGURE 3. **Cav-1 knockdown does not alter TRPC3 and IP_3R1 expression in cerebral arteries.** *A*, representative Western blot illustrating that cav-1shV induces knockdown of cav-1, but does not alter IP_3R1 or TRPC3 expression. *B*, mean data illustrating effects of cav-1shV on TRPC3 and IP_3R1 protein ($n = 4$ for each; *, $p < 0.05$).

CSD Peptide Attenuates IP_3-induced I_{Cat} Activation and Vasoconstriction—The cav-1 N terminus contains a CSD that interacts with and regulates a wide variety of signaling proteins containing a CSD-interacting motif (25, 26). CSD-interacting motifs are characterized as $\Phi X\Phi XXXX\Phi$ and $\Phi XXXX\Phi XX\Phi$, where Φ is a tryptophan, phenylalanine, or

tyrosine, and *X* is any amino acid (26). As shown in Fig. 5*A*, the N and C termini of IP_3R1 and the C terminus of TRPC3 channels contain CSD-binding motifs, suggesting that IP_3R1 and TRPC3 channels may both interact with cav-1.

To study the physiological function of the CSD in IP_3-induced I_{Cat} activation and vasoconstriction, we used a synthetic peptide corresponding to the cav-1 CSD sequence (amino acids 82–101, DGIWKASFTTFTVTKYWFYR). This CSD peptide competes with endogenous cav-1 for interacting protein binding. CSD peptide was conjugated to an antennapedia (ANT) internalization sequence (ANT-CSD, amino acids 43–58, RQIKIWFQNRRMKWKK) to improve membrane permeability. An ANT peptide was used as an experimental control. To examine membrane permeability of the peptide, a FITC-labeled ANT peptide (ANT-FITC) was used. Confocal imaging of arteries exposed to ANT-FITC indicated successful introduction into smooth muscle cells (Fig. 5*B*).

ANT-CSD peptide did not alter smooth muscle cell capacitance (ANT *versus* ANT-CSD, 12 ± 2 *versus* 11 ± 1 pF, $n = 5$ and 6, respectively, $p > 0.05$). However, ANT-CSD peptide reduced IP_3-induced I_{Cat} density by ~48% when compared with control (ANT; Fig. 5, *C* and *D*). ANT-CSD peptide did not alter myogenic tone in endothelium-denuded pressurized (60 mmHg) cerebral arteries (ANT *versus* ANT-CSD, ~22 ± 6 *versus* 20 ± 3%, $n = 6$ and 5, respectively, $p > 0.05$). In contrast, ANT-CSD peptide attenuated IP_3-induced vasoconstriction by ~61% in pressurized (60 mmHg) cerebral arteries (Fig. 6, *A* and *B*). These data indicate that the CSD regulates IP_3-induced I_{Cat} activation in arterial smooth muscle cells and IP_3-induced vasoconstriction in pressurized arteries.

Cerebral Artery cav-1 Immunoprecipitates with Both TRPC3 and IP_3R1—To test the hypothesis that cav-1 exists in a macromolecular protein complex with IP_3R1 and TRPC3 channels, co-IP was performed. A cav-1 antibody co-immunoprecipitated cav-1, IP_3R1, and TRPC3 from cerebral artery lysate (Fig. 7). These data indicate that cav-1, IP_3R1, and TRPC3 channels are located within the same macromolecular complex in cerebral arteries.

Cav-1 and TRPC3 Are Spatially Localized in Arterial Smooth Muscle Cells—Spatial localization of TRPC3 channels to cav-1 in arterial smooth muscle cells was studied using immunoFRET. Fig. 8*A* indicates that cav-1 and TRPC3 are co-localized in the arterial smooth muscle cell plasma membrane. Alexa 488- and Alexa 546-conjugated secondary antibodies bound to cav-1 and TRPC3 channel primary antibodies, respectively, generated mean N-FRET of 23.0 ± 1.2% ($n = 16$). These data indicate that cav-1 and TRPC3 are spatially localized in the cerebral artery smooth muscle cell plasma membrane.

IP_3R1 and TRPC3 Are in Located in Close Spatial Proximity and Separated by Caveolae Disruption or CSD Peptide in Arterial Smooth Muscle Cells—ImmunoFRET was also used to measure the spatial proximity of IP_3R1 and TRPC3 channels

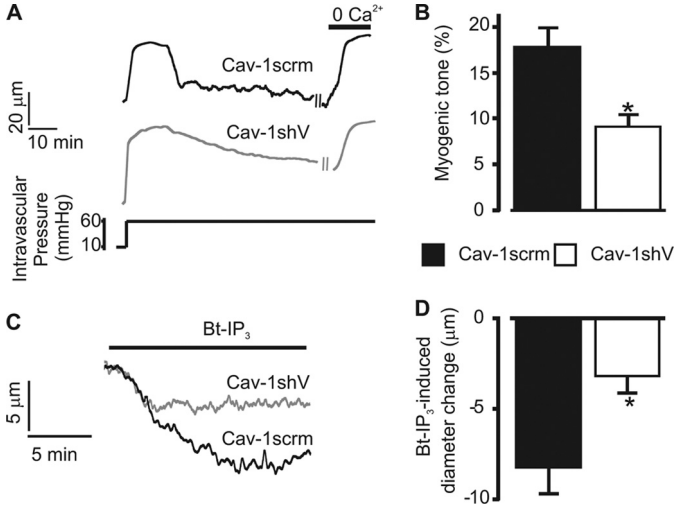

FIGURE 4. **Cav-1 knockdown attenuates myogenic tone and IP_3-induced vasoconstriction in cerebral arteries.** *A*, representative recordings illustrating that cav-1 knockdown attenuates myogenic tone in endothelium-denuded arteries. *B*, mean myogenic tone in cav-1scrm ($n = 4$)- and cav-1shV ($n = 5$)-treated arteries. *C*, representative traces illustrating Bt-IP_3 (10 nM)-induced vasoconstriction in cav-1scrm and cav-1shV-treated cerebral arteries. *D*, mean Bt-IP_3-induced vasoconstriction in cav-1scrm (control; $n = 4$)- or cav-1shV ($n = 5$)-treated arteries. *, $p < 0.05$ when compared with cav-1scrm.

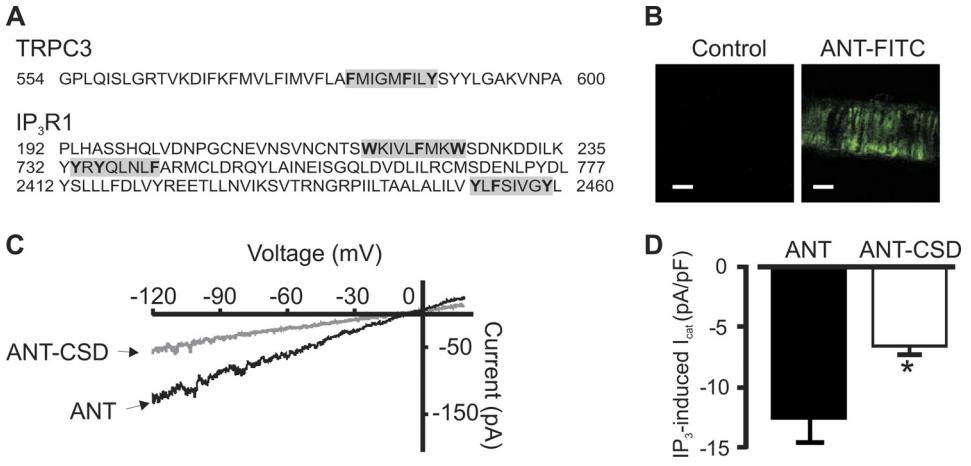

FIGURE 5. **CSD peptide attenuates IP_3-induced I_{Cat} activation in cerebral artery smooth muscle cells.** *A*, C terminus of TRPC3 and N and C termini of IP_3R1 contain CSD binding sequences (highlighted in *gray*). *Bold letters* indicate tryptophan, phenylalanine, or tyrosine. *B*, fluorescent images indicating successful introduction of FITC-labeled ANT peptide into smooth muscle cells of cerebral arteries. *C*, representative recordings illustrating that ANT-CSD peptide (50 μM) attenuates IP_3 (10 μM)-induced I_{Cat} activation in arterial smooth muscle cells. *D*, mean IP_3 -induced I_{Cat} activation in ANT (control; $n = 5$)- and ANT-CSD ($n = 6$) peptide-treated cells. *, $p < 0.05$ when compared with ANT. Scale bar, 50 μm.

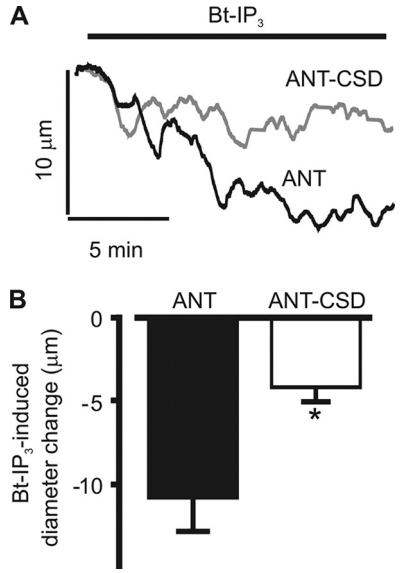

FIGURE 6. **CSD peptide attenuates IP_3-induced vasoconstriction in pressurized cerebral arteries.** *A*, representative traces illustrating that ANT-CSD peptide attenuates Bt-IP_3 (10 nM)-induced vasoconstriction. *B*, mean Bt-IP_3-induced vasoconstriction in arteries treated with ANT ($n = 6$) and ANT-CSD ($n = 5$) peptides. *, $p < 0.05$ when compared with ANT.

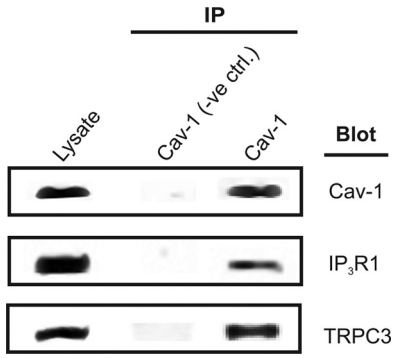

FIGURE 7. **Cav-1 antibody co-immunoprecipitates cerebral artery cav-1 (~22 kDa), IP_3R1 (~270 kDa), and TRPC3 (~90 kDa).** Lysate supernatant (~40 μg of protein) was used as the input control. Negative control (*-ve ctrl.*) received the same concentration of cav-1 antibody except that the coupling resin was replaced with control agarose resin that is not amine-reactive.

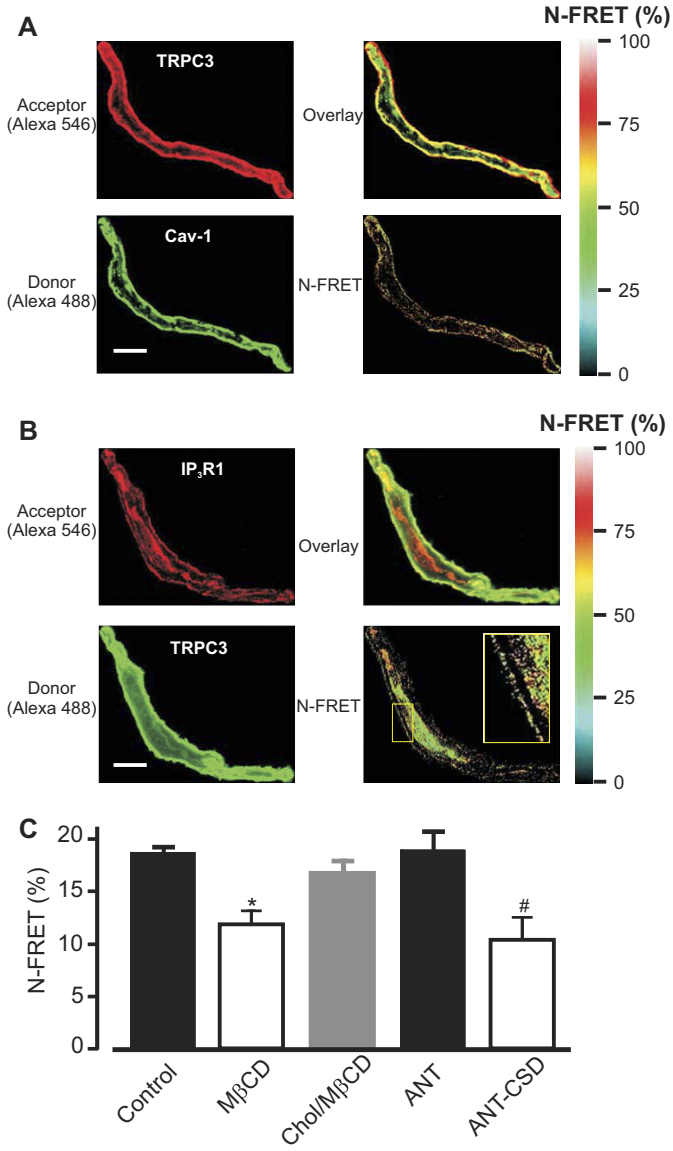

FIGURE 8. **Spatial co-localization of cav-1, IP_3R1, and TRPC3 and modulation by caveolae disruption and CSD peptide in cerebral artery smooth muscle cells.** *A*, confocal images illustrating localization of cav-1 and TRPC3 channels in an arterial smooth muscle cell. Shown are fluorescent images generated by Alexa 546- and 488-conjugated antibodies, pixel overlay, and N-FRET in the same cell. *B*, confocal images illustrating cellular locations of IP_3R1 and TRPC3 in a control cell. Images show the overlay and FRET generated by secondary antibodies bound to these proteins in the same control cell. The *inset* in *panel 4* is a magnified view of the *boxed area* of the cell showing FRET localization to the plasma membrane. *C*, mean N-FRET data for IP_3R1 and TRPC3 for control ($n = 16$), MβCD (5 mM, 30 min, $n = 11$), reversal of MβCD effect by Chol/MβCD (100 μg/ml, 1 h, $n = 13$), ANT (50 μM, 1 h, $n = 8$), and ANT-CSD peptide (50 μM, 1 h, $n = 10$). *, $p < 0.05$ when compared with control; #, $p < 0.05$ when compared with ANT. *Scale bars*, 10 μm.

in arterial smooth muscle cells. Alexa 488- and Alexa 546-labeled secondary antibodies bound to TRPC3 channel and IP_3R1 primary antibodies, respectively, generated mean N-FRET of ~19% (Fig. 8, *B* and *C*). Fig. 8*B* illustrates that immunoFRET was localized both to the plasma membrane and intracellularly. MβCD treatment and ANT-CSD peptide reduced mean N-FRET to ~12 and 10%, respectively (Fig. 8*C*). The MβCD-induced reduction in N-FRET was reversed by subsequent exposure of MβCD-treated cells to Chol/MβCD (Fig. 8*C*). These data indicate that caveolae and the cav-1 CSD maintain IP_3R1 and TRPC3 in close spatial proximity in arterial smooth muscle cells.

DISCUSSION

Data in this study indicate that cav-1 maintains IP_3R1 and TRPC3 channels in a signaling complex that enables IP_3-induced I_{Cat} activation and vasoconstriction in cerebral artery smooth muscle cells. We show that: 1) caveolae disassembly reduces myogenic tone and attenuates IP_3-induced I_{Cat} activation and vasoconstriction, 2) cav-1 knockdown does not alter IP_3R1 and TRPC3 channel expression but reduces myogenic tone and IP_3-induced vasoconstriction, 3) the N and C termini of IP_3R1 and the C terminus of TRPC3 contain CSD-interacting motifs, 4) a CSD peptide inhibits IP_3-induced I_{Cat} activation and vasoconstriction, 5) cav-1, IP_3R1 and TRPC3 are located within the same macromolecular complex in cerebral arteries, and 6) the close spatial proximity of IP_3R1 and

TRPC3 is disrupted by caveolae disassembly and a CSD peptide. In summary, data indicate that that cav-1 and caveolae spatially localize IP_3R1 and TRPC3 channels in cerebral artery smooth muscle cells, enabling IP_3-induced physical coupling, leading to I_{Cat} generation and vasoconstriction.

Three IP_3R isoforms (1–3) have been cloned (27, 28). IP_3R1 is the primary molecular and functional isoform expressed in arterial smooth muscle cells (6). In cerebral artery smooth muscle cells, plasma membrane TRPC3 channels are located in close spatial proximity to IP_3R1 (4). IP_3 activates plasma membrane TRPC3 channels by inducing a direct interaction between the IP_3R1 N terminus and TRPC3 channel calmodulin and IP_3R binding (CIRB) domains (4). IP_3-induced TRPC3 channel activation causes Na^+ influx, resulting in membrane depolarization, voltage-dependent Ca^{2+} channel activation, an intracellular Ca^{2+} ($[Ca^{2+}]_i$) elevation, and vasoconstriction. Therefore, IP_3R1 and TRPC3 channels directly couple in arterial smooth muscle cells (4, 5).

Several TRP channels, including TRPC3, localize within caveolae in mammalian cells (29). Such localization may enhance TRP channel interaction with other cell signaling molecules (29). However, whether caveolae localize TRPC3 channels nearby other regulatory proteins in arterial smooth muscle cells was unclear. Our data indicate that cav-1 and TRPC3 are spatially localized in the arterial smooth muscle cell plasma membrane, suggesting that TRPC3 may be localized in caveolae. In rat tail arteries and pulmonary artery smooth muscle cells, cholesterol depletion by MβCD reduced caveolae density and altered plasma membrane morphology, and these effects were reversed by cholesterol replenishment (15, 23). To examine a role for caveolae and cav-1 in enabling functional IP_3R1 to TRPC3 channel physical coupling in arterial smooth muscle cells, we used MβCD at concentrations previously utilized to effectively disrupt plasma membrane caveolae (15, 23, 30, 31). MβCD reduced smooth muscle cell membrane capacitance and this was reversed by subsequent cholesterol treatment. Reduced cell capacitance has also been reported in arterial smooth muscle cells lacking cav-1, and in MβCD-treated uterine and urinary bladder smooth muscle cells (13, 32, 33). These studies and ours indicate that acute and chronic loss of caveolae reduces smooth muscle cell surface area. In another previous study, MβCD-mediated caveolae disruption did not alter arterial smooth muscle cell membrane capacitance (34). Reasons for these contradictory observations are unclear. MβCD modulates depolarization of skinned skeletal muscle fibers (35). However, MβCD treatment did not alter membrane potential or basal intracellular Ca^{2+} concentration in cerebral artery smooth muscle cells (34). These studies suggest that the effect of MβCD on membrane potential may be cell type-dependent. Here, MβCD and cav-1 knockdown attenuated myogenic constriction in cerebral arteries, consistent with observations in cerebral and mesenteric arteries from cav-1 knock-out mice and MβCD-treated rat mesenteric arteries (16, 17, 30). It is unclear why MβCD and cav-1 knockdown reduced myogenic tone, whereas the CSD peptide did not alter myogenic tone. One explanation may be that cav-1 regulates myogenic tone via a CSD-independent mechanism. Alternatively, the CSD peptide used may more effectively block physical coupling of IP_3R1 to TRPC3 channels than it inhibits CSD-dependent mechanisms that lead to cerebral artery myogenic constriction.

We demonstrate for the first time that caveolae disassembly and a CSD peptide reduces IP_3-induced I_{Cat} activation in smooth muscle cells and vasoconstriction in pressurized arteries. Co-IP data demonstrated that cav-1, IP_3R1, and TRPC3 channels are contained within the same macromolecular complex in cerebral arteries. We also show that both IP_3R1 and TRPC3 channels contain CSD binding motifs. The CSD peptide did not alter smooth muscle cell capacitance, suggesting that caveolae integrity and thus, cell surface area remained unchanged. However, the CSD peptide attenuated IP_3-induced I_{Cat} activation in smooth muscle cells and vasoconstriction in pressurized arteries. We tested the hypothesis that caveolae/cav-1 spatially localize plasma membrane TRPC3 channels nearby SR membrane IP_3R1 channels, thereby permitting physical coupling of these proteins. The Förster distance between Alexa 488 and 546 is 6.4 nm (Invitrogen). Given that secondary antibodies bound to IP_3R1 (Alexa 546) and TRPC3 (Alexa 488) generated significant N-FRET, these data indicate that IP_3R1 and TRPC3 channels are located in very close spatial proximity. Our data indicate that FRET was localized both at the plasma membrane and within the cytosol. Intracellular protein complexes containing both IP_3Rs and TRPC3 have previously been reported in HEK-293 cells (36). We have also previously shown that a proportion of TRPC3 protein is intracellular in rat cerebral arteries and that TRPC3 immunofluorescence exhibits both plasma membrane and intracellular localization in arterial smooth muscle cells (4). Conceivably, intracellular TRPC3 channels may be located on organelle membranes that are nearby SR IP_3R1 channels or stored within the SR prior to trafficking and in close proximity to SR IP_3R1. Caveolae disruption and the CSD peptide both reduced the IP_3R1/TRPC3 N-FRET signal, indicating that these proteins became spatially separated. These data indicate that cav-1, IP_3R1 and TRPC3 channels form a macromolecular complex. Additional data indicate that this complex enables physically coupling of SR IP_3R1 to plasma membrane TRPC3 channels thereby allowing direct communication between intracellular and plasma membrane proteins. MβCD and CSD peptide reduced IP_3-induced I_{Cat} and MβCD, CSD peptide, and cav-1 knockdown attenuated IP_3-induced vasoconstriction. Therefore, cav-1 and caveolae enable IP_3R1 to physically couple to TRPC3 channels in smooth muscle cells to control arterial diameter.

Recombinant cav-1 interacts with both endogenous IP_3R3 and recombinant TRPC1 in HEK-293 cells (37). Expression of a CSD-deleted cav-1 mutant in HEK-293 cells and a human dermal microvascular endothelial cell line increased store-operated Ca^{2+}entry (SOCE) and attenuated a thapsigargin-induced IP_3R3-TRPC1 interaction in HEK-293 cells (37). These studies suggested that through its scaffolding domain, cav-1 regulates an IP_3R3-TRPC1 complex and SOCE in cultured HEK-293 and endothelial cells (37, 38). Store-operated cation currents have been described in a variety of vascular smooth muscle cells, including aorta, mesenteric artery, and portal vein (39). In contrast, SR Ca^{2+} depletion does not acti-

vate a I_{Cat} or alter IP_3-induced I_{Cat} activation in cerebral artery smooth muscle cells or modify IP_3- and agonist-induced cerebral artery constriction at low intravascular pressure (5, 6). SR Ca^{2+} depletion also did not induce contraction in cerebral arteries at low or no pressure (5, 40, 41). Collectively, these studies indicate that SOCE does not appear to exist in contractile cerebral artery smooth muscle cells.

In conclusion, we demonstrate that cav-1 maintains IP_3R1 and TRPC3 channels in a functional macromolecular complex in cerebral artery smooth muscle cells. Cav-1 enables IP_3 to stimulate physical coupling between IP_3R1 and TRPC3 channels, leading to I_{Cat} activation and vasoconstriction.

REFERENCES

1. Berridge, M. J. (1993) *Nature* **361,** 315–325
2. Sanders, K. M. (2001) *J. Appl. Physiol.* **91,** 1438–1449
3. Albert, A. P., Saleh, S. N., and Large, W. A. (2009) *Curr. Med. Chem.* **16,** 1158–1165
4. Adebiyi, A., Zhao, G., Narayanan, D., Thomas-Gatewood, C. M., Bannister, J. P., and Jaggar, J. H. (2010) *Circ. Res.* **106,** 1603–1612
5. Xi, Q., Adebiyi, A., Zhao, G., Chapman, K. E., Waters, C. M., Hassid, A., and Jaggar, J. H. (2008) *Circ. Res.* **102,** 1118–1126
6. Zhao, G., Adebiyi, A., Blaskova, E., Xi, Q., and Jaggar, J. H. (2008) *Am. J. Physiol. Cell Physiol.* **295,** C1376–C1384
7. Liu, M., Albert, A. P., and Large, W. A. (2005) *J. Physiol.* **566,** 161–171
8. Bray, D. (1998) *Annu. Rev. Biophys. Biomol. Struct.* **27,** 59–75
9. Razani, B., Woodman, S. E., and Lisanti, M. P. (2002) *Pharmacol. Rev.* **54,** 431–467
10. Zhao, Y. Y., Liu, Y., Stan, R. V., Fan, L., Gu, Y., Dalton, N., Chu, P. H., Peterson, K., Ross, J., Jr., and Chien, K. R. (2002) *Proc. Natl. Acad. Sci. U.S.A.* **99,** 11375–11380
11. Drab, M., Verkade, P., Elger, M., Kasper, M., Lohn, M., Lauterbach, B., Menne, J., Lindschau, C., Mende, F., Luft, F. C., Schedl, A., Haller, H., and Kurzchalia, T. V. (2001) *Science* **293,** 2449–2452
12. Razani, B., Engelman, J. A., Wang, X. B., Schubert, W., Zhang, X. L., Marks, C. B., Macaluso, F., Russell, R. G., Li, M., Pestell, R. G., Di Vizio, D., Hou, H., Jr., Kneitz, B., Lagaud, G., Christ, G. J., Edelmann, W., and Lisanti, M. P. (2001) *J. Biol. Chem.* **276,** 38121–38138
13. Cheng, X., and Jaggar, J. H. (2006) *Am. J. Physiol. Heart Circ. Physiol.* **290,** H2309–H2319
14. Je, H. D., Gallant, C., Leavis, P. C., and Morgan, K. G. (2004) *Am. J. Physiol. Heart Circ. Physiol.* **286,** H91–H98
15. Dreja, K., Voldstedlund, M., Vinten, J., Tranum-Jensen, J., Hellstrand, P., and Swärd, K. (2002) *Arterioscler. Thromb. Vasc. Biol.* **22,** 1267–1272
16. Shaw, L., Sweeney, M. A., O'Neill, S. C., Jones, C. J., Austin, C., and Taggart, M. J. (2006) *Cardiovasc. Res.* **69,** 825–835
17. Adebiyi, A., Zhao, G., Cheranov, S. Y., Ahmed, A., and Jaggar, J. H. (2007) *Am. J. Physiol. Heart Circ. Physiol.* **292,** H1584–H1592
18. Jaggar, J. H. (2001) *Am. J. Physiol.* **281,** C439–C448
19. Adebiyi, A., McNally, E. M., and Jaggar, J. H. (2008) *Mol. Pharmacol.* **74,** 736–743
20. Lesh, R. E., Somlyo, A. P., Owens, G. K., and Somlyo, A. V. (1995) *Circ. Res.* **77,** 220–230
21. Morgan, J. P., DeFeo, T. T., and Morgan, K. G. (1984) *Pflugers Arch.* **400,** 338–340
22. Xia, Z., and Liu, Y. (2001) *Biophys. J.* **81,** 2395–2402
23. Patel, H. H., Zhang, S., Murray, F., Suda, R. Y., Head, B. P., Yokoyama, U., Swaney, J. S., Niesman, I. R., Schermuly, R. T., Pullamsetti, S. S., Thistlethwaite, P. A., Miyanohara, A., Farquhar, M. G., Yuan, J. X., and Insel, P. A. (2007) *FASEB J.* **21,** 2970–2979
24. Christian, A. E., Haynes, M. P., Phillips, M. C., and Rothblat, G. H. (1997) *J. Lipid Res.* **38,** 2264–2272
25. Li, S., Okamoto, T., Chun, M., Sargiacomo, M., Casanova, J. E., Hansen, S. H., Nishimoto, I., and Lisanti, M. P. (1995) *J. Biol. Chem.* **270,** 15693–15701
26. Okamoto, T., Schlegel, A., Scherer, P. E., and Lisanti, M. P. (1998) *J. Biol. Chem.* **273,** 5419–5422
27. Blondel, O., Takeda, J., Janssen, H., Seino, S., and Bell, G. I. (1993) *J. Biol. Chem.* **268,** 11356–11363
28. Ross, C. A., Danoff, S. K., Schell, M. J., Snyder, S. H., and Ullrich, A. (1992) *Proc. Natl. Acad. Sci. U.S.A.* **89,** 4265–4269
29. Ambudkar, I. S., Brazer, S. C., Liu, X., Lockwich, T., and Singh, B. (2004) *Novartis Found. Symp.* **258,** 63–70
30. Dubroca, C., Loyer, X., Retailleau, K., Loirand, G., Pacaud, P., Feron, O., Balligand, J. L., Lévy, B. I., Heymes, C., and Henrion, D. (2007) *Cardiovasc. Res.* **73,** 190–197
31. Potocnik, S. J., Jenkins, N., Murphy, T. V., and Hill, M. A. (2007) *J. Vasc. Res.* **44,** 292–302
32. Shmygol, A., Noble, K., and Wray, S. (2007) *J. Physiol.* **581,** 445–456
33. Hotta, S., Yamamura, H., Ohya, S., and Imaizumi, Y. (2007) *J. Pharmacol. Sci.* **103,** 121–126
34. Löhn, M., Furstenau, M., Sagach, V., Elger, M., Schulze, W., Luft, F. C., Haller, H., and Gollasch, M. (2000) *Circ. Res.* **87,** 1034–1039
35. Launikonis, B. S., and Stephenson, D. G. (2001) *J. Physiol.* **534,** 71–85
36. Kim, J. Y., Zeng, W., Kiselyov, K., Yuan, J. P., Dehoff, M. H., Mikoshiba, K., Worley, P. F., and Muallem, S. (2006) *J. Biol. Chem.* **281,** 32540–32549
37. Sundivakkam, P. C., Kwiatek, A. M., Sharma, T. T., Minshall, R. D., Malik, A. B., and Tiruppathi, C. (2009) *Am. J. Physiol. Cell Physiol.* **296,** C403–C413
38. Kwiatek, A. M., Minshall, R. D., Cool, D. R., Skidgel, R. A., Malik, A. B., and Tiruppathi, C. (2006) *Mol. Pharmacol.* **70,** 1174–1183
39. Albert, A. P., Saleh, S. N., Peppiatt-Wildman, C. M., and Large, W. A. (2007) *J. Physiol.* **583,** 25–36
40. Flemming, R., Cheong, A., Dedman, A. M., and Beech, D. J. (2002) *J. Physiol.* **543,** 455–464
41. Bergdahl, A., Gomez, M. F., Wihlborg, A. K., Erlinge, D., Eyjolfson, A., Xu, S. Z., Beech, D. J., Dreja, K., and Hellstrand, P. (2005) *Am. J. Physiol. Cell Physiol.* **288,** C872–C880